J Mater Sci (2008) 43:5579–5584
DOI 10.1007/s10853-008-2803-y

Induced effect of transparent substrate composition on polypyrrole thin film

D. Martel · H. Nguyen Cong · J. L. Gautier

Received: 14 March 2008 / Accepted: 11 June 2008 / Published online: 8 July 2008

Abstract For thin films of tin dioxide, indium oxide and indium tin oxide, the substrate nature plays a determining role on their structural and morphological characteristics, which modified noticeably their optical property. On these substrates, the electropolymerization characteristics of polypyrrole exhibited the profound modifications related to the active sites for nuclei formation and their growth. These modifications induced the important change in charge transport characteristics of polypyrrole thin films.

Introduction

The high stability, good conductivity and simple preparation from aqueous solution have rendered polypyrrole (PPy) as one of conjugated conducting polymers the most attractive for various applications in batteries [1, 2], anticorrosion, electrochromic devices [3], electrocatalysis [4–6] and sensors [7–9]. Previous works have pointed out the feasibility of multilayered PPy/Ox composite electrodes in which Ox was spinel oxide nanoparticles of copper and manganese $Cu_{1.4}Mn_{1.6}O_4$ or of nickel and cobalt $Ni_xCo_{3-x}O_4$, dispersed and confined in an inner PPy/Ox layer sandwiched between two PPy layers [10, 11]. Such electrodes exhibit excellent electrocatalytic reactivity towards oxygen reduction reaction [12, 13] with remarkable stability [14].

On the other hand, the lower oxidation of pyrrole (Py) compared to other monomers offers the possibility of PPy films formation on different substrates, not only on chemically inert materials (Au, Pt, glassy carbon) [15, 16], but also on active metal (iron, mild steel) [17, 18] and on semiconducting transparent substrates, such as indium tin oxide (ITO) and tin dioxide (SnO_2), [19, 20] as well as. However, no work concerning the correlation between the characteristics of PPy films and substrates nature has been reported.

According to some authors [21], the presence of PPy on Pt substrate modifies noticeably its electrochemical behaviour. On semiconducting transparent substrates, such as ITO, In_2O_3 and SnO_2, the presence of PPy submonolayers plays a determining role on the adsorption characteristics of polyoxometalate, as reported in recent work [22]. Such modification can be attributed to the changes of surface characteristics involved by PPy submonolayer formation. This study [22] reveals a promising self-assembly property between polyoxometalate and PPy films on SnO_2. This can be used to prepare complicated multilayer thin films by self-assembly.

It is well known that the charge transport properties of counter ions inside of PPy films depend strongly upon electropolymerization parameters (nature and concentration of doping anions, substrate nature) [23–26]. These properties, as one can expect, play a determining role on self-assembly properties and reactivity electrocatalytical of composite electrodes based on PPy films.

D. Martel (✉) · H. Nguyen Cong (✉)
Laboratoire d'Electrochimie et de Chimie Physique du Coprs Solide, LC3 – UMR7177, CNRS-Université Louis Pasteur, 4 Rue Blaise Pascal, 67000 Strasbourg, France
e-mail: dmartel@chimie.u-strasbg.fr

H. Nguyen Cong
e-mail: hnguyen@chimie.u-strasbg.fr

J. L. Gautier
Laboratorio de Fisicoquímica y Electroquímica de Sólidos, Departamento de Química de los Materiales, Facultad de Química y Biología, Universidad de Santiago de Chile, Av. L. B. O'Higgins 3363, Santiago, Chile

The aim of this work is to investigate the correlations between the properties of PPy thin films and substrate nature.

Experimental

Materials

The potassium chloride and the pyrrole were purchased from Aldrich Chemical Co. Pyrrole was distilled prior to use and potassium chloride used as received. The pyrrole (Py) monomer was dissolved at a concentration of 0.25 M in a 0.50 M ultra pure water solution of KCl. This solution was stored under argon atmosphere at 4 °C in the dark before it was used. The semi-conducting oxides working electrodes were glass piece of 1 cm × 2 cm covered by the oxide layer of about 400 nm thickness and having the structure G/S, where G corresponds to glass and S represents In_2O_3, ITO or SnO_2. The In_2O_3 and ITO substrates were purchased from Diamond Coatings Limited Company (UK), from Sagem (Fr), respectively. Concerning SnO_2 one, the spray pyrolysis method was used to obtain a conductive and low cost substrate. This technique consists of spraying at room temperature an aqueous or organic solution of metallic salts using a usually inert gas vector on an appropriate substrate heated at a selected temperature. On the surface of the substrate the thermal decomposition occurs and the solvent evaporates from the droplets while a chemical process leads to the formation of a solid thin film.

The experimental set-up and spraying procedure have been previously described in detail [27–29]. In this work, the circular movement of spray gun is 25 rpm (instead of 10 rpm).

In order to prepare SnO_2 electrodes, we used Pyrex glass slides as substrate (1 cm × 2 cm) which were previously mechanically and smoothly polished. One side was roughened with carborundum 450, to ensure good adherence and a better temperature distribution. In order to clean the glass surfaces, they were immersed in warm (60 °C) 1 M HNO_3 + 1 M HCl solution for 3 min, rinsed thoroughly with bidistilled water and then degreased in hot acetone. After that they were etched for 5 min in boiling 10% oxalic acid, washed in bidistilled water and finally cleaned ultrasonically in bidistilled water.

An inert interlayer of tin oxide doped with fluorine (SnO_2:F films) was deposited by spray pyrolysis to obtain conductive glasses. The optimal conditions of preparation were carefully determined elsewhere [29]. Optimized conductive layers were obtained by spraying methanolic solutions 0.2 M in $SnCl_4$ and 0.14 M in NH_4F at a flow rate of 4 mL min^{-1} onto a hot (430 °C) roughened glass slide. The vector gas was air at a pressure of 2 bars. All reagents were analytical grade ($SnCl_4$ and NH_4F, Prolabo; CH_3OH, Merck). The temperature of the substrate was checked with an infrared pyrometer Cyclops 330 (Minolta). The spraying rate of the solution was regulated with a peristaltic pump.

Electrochemistry

The PPy films involve the electropolymerization of pyrrole in a one compartment cell containing 18 mL of 0.5 M KCl + 0.25 M Py solution. The G/S substrates were working electrodes with 1 cm^2 surface area. Prior to electropolymerization, they were rinsed with ethanol then washed with doubly distilled water in an ultrasonic bath. The counter and reference electrodes were a Pt plate and a saturated calomel electrode (SCE), respectively. The electrolyte solution was deoxygenated for 30 min before use by bubbling Ar and maintained under Ar atmosphere during electropolymerization of pyrrole. The PPy electrodeposition was performed at room temperature at a constant potential $E = 1.2$ V/SCE for 70 s using an Autolab PGSTAT 20 potentiostat equipped with a data acquisition system.

Cyclic voltammetry experiments were carried out at ambient temperature (20 ± 2 °C) in a two compartments cell, using the same Autolab model PGSTAT 20 potentiostat as above. The aqueous electrolyte of 0.5 M KCl solution in absence of Py monomer was bubbled with argon during 30 min prior to use and maintained under Ar atmosphere during the experiment. All potentials were measured versus a commercial (Tacussel) calomel reference electrode (SCE) (KCl sat.). The platinum wire used as auxiliary electrode was placed in a separate compartment in order to avoid contamination of the electrolytic solution by electrogenerated species. The working electrodes G/S were rinsed with doubly distilled water and dried under argon.

Instrumentation

The structure of different substrates was determined by X-ray diffraction (XRD) with a Siemens D500 diffractometer using CoK_α radiation. Their morphology was characterized by scanning electron microscope Jeol JMS 840 and the actual metal ratio in oxides was checked by EDAX. The optical properties of substrates and PPy films were characterized by UV–Vis absorption spectra recorded by a mono beam HP-Agilent 8453 spectrophotometer.

Results and discussion

Substrates characterization

The XRD spectra recorded on In_2O_3, ITO and SnO_2 substrates were shown in Fig. 1. They show a strong similarity between XRD data recorded on SnO_2 prepared by spray pyrolysis and

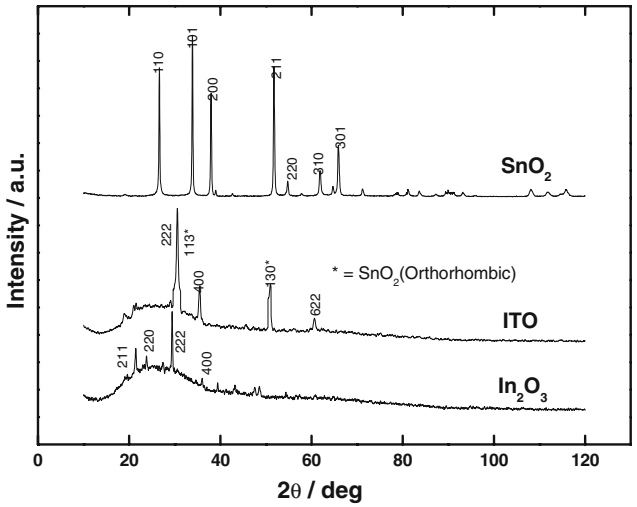

Fig. 1 X-ray diffraction patterns of SnO_2, ITO and In_2O_3

those reported in ASTM Power Diffraction File for this compound (41-1445 File). This indicates that this substrate exhibits a tetragonal structure with a (101) preferential crystallographic plane which is different than that reported for the selected ASTM compound. This discrepancy results probably from the preparation methods. The high crystallization of this compound allows to estimate its *a* and *c* tetragonal cell parameters which are 4.74 and 3.18 Å, respectively. In case of In_2O_3, its crystallization degree is rather poor. The main peak was found to corresponds to (222) crystallographic plane of centred cubic system (06-0416 File). Concerning ITO, the EDAX analysis pointed out that Sn/In ratio in this compound was closed to 0.22. For such compound, taking into account the unavailability of ASTM power diffraction file on the one hand and the XRD results (Fig. 1) on the other hand, one can suggest that the Sn incorporation into In_2O_3 leads to a solid solution formation in which the In_2O_3 structure remains unchanged, while SnO_2 having an orthorhombic structure (ASTM, 78-1063 File) seems improve crystallization of In_2O_3. These results are supported by microphotographs performed on these substrates, as shown in Fig. 2. It can be seen a very smooth morphology was obtained for In_2O_3 (Fig. 2a), while a less regular texture was observed on ITO (Fig. 2b). This indicates that roughnesses begin to develop onto ITO solid solution, which result likely from the high crystallization degree of SnO_2 (Fig. 1). This hypothesis is confirmed by the occurrence of very sharp morphology for SnO_2, where only the big crystallites with well definite structure were observed (Fig. 2c).

The Fig. 3 displays the transmission spectra recorded on In_2O_3, ITO and SnO_2 bare substrates. They pointed out a great difference in optical behaviours of these substrates. Indeed, the spectrum performed on In_2O_3 shows in 400 nm region an absorption edge more abrupt than those of ITO and SnO_2 substrates, and reveals the striking oscillations

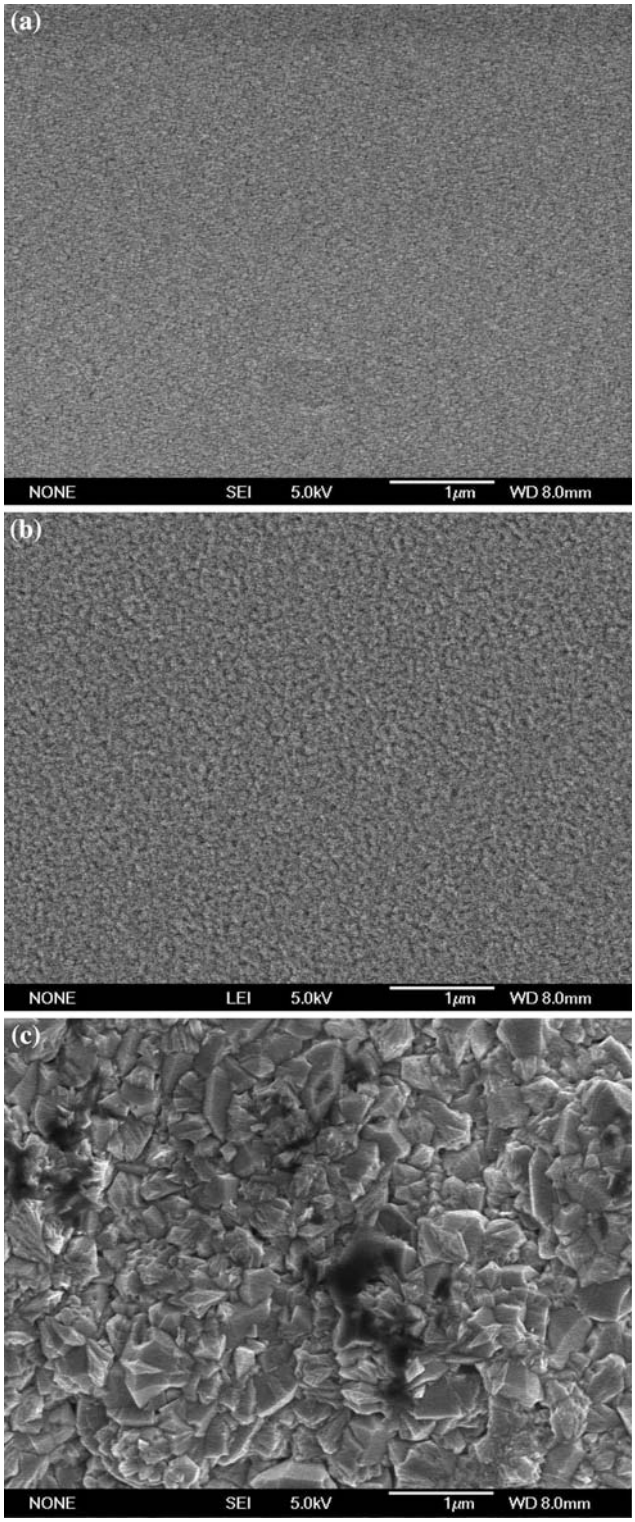

Fig. 2 Morphology of In_2O_3 (**a**), ITO (**b**) and SnO_2 (**c**)

which reduced strongly on ITO and practically vanished for the case of SnO_2. A similar fact was reported for CdS thin films obtained by thermal evaporation in vacuum [30]. Such oscillations resulted from Fabry-Perot interference fringes regenerated by two flat surfaces in parallel with a

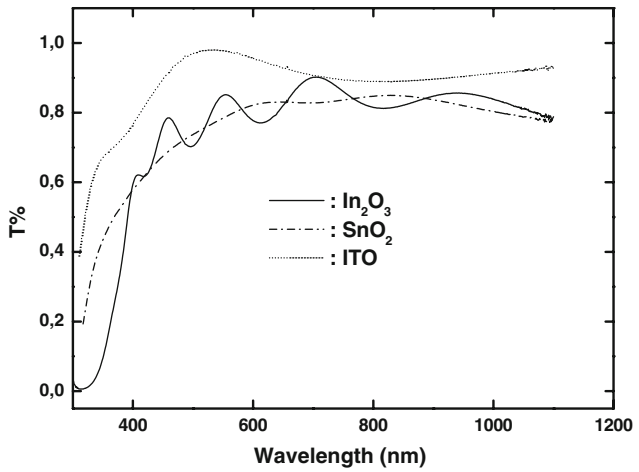

Fig. 3 Transmission spectra of various substrates

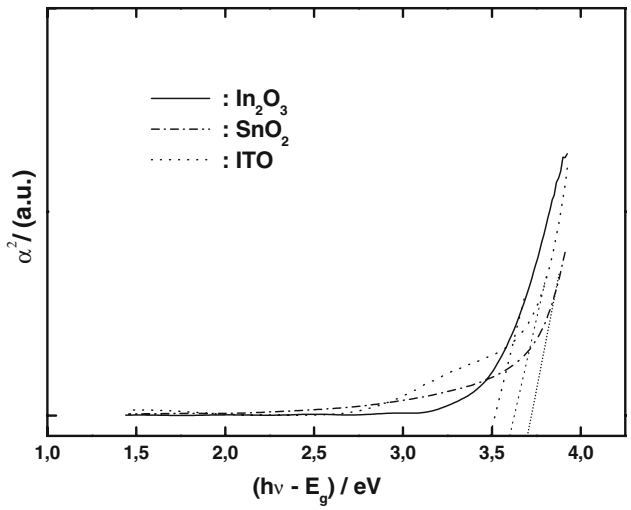

Fig. 4 Variation of absorption coefficient, α^2, function of photon energy, $h\nu$, from data in Fig. 3

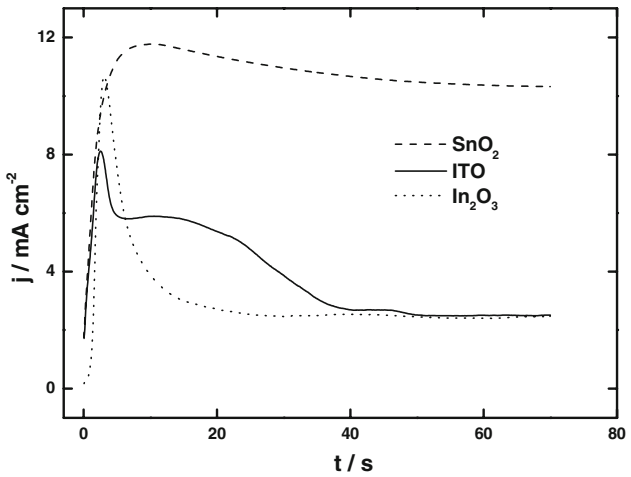

Fig. 5 Chronoamperometric curves related to Py electropolymerization on various substrates, in 0.25 M Py + 0.50 M KCl solution previously deoxygenated, at room temperature, $E = 1.2$ V/SCE

low distance between them. In case of In_2O_3, its very smooth surface, as shown in Fig. 2a, allows to suggest that the surface of this compound and glass one are in parallel. Consequently, the oscillations occurred. Concerning ITO, this compound is a solid solution of In_2O_3 and of SnO_2 as shown in Fig. 1. The presence of latter with an orthorhombic structure reduces the surface quality of ITO (Fig. 2b) due to the micro-crystallites formation which lead to a decrease of parallelism between its surface and support one. The occurrence of oscillations diminishes. About SnO_2 case with big crystallites (Fig. 2c), its surface quality does totally not satisfy Fabry-Perot requirements. For this reason, oscillations are practically vanished. The Fig. 3 results allowed to determine the bandgap, E_g, of these oxides, as shown in Fig. 4, using the relation reported for materials with direct gap [31]:

$$(\alpha h\nu)^2 = A(h\nu - E_g)$$

where α is the absorption coefficient, $h\nu$ is the photon energy and A is a constant.

The E_g were 3.49, 3.60 and 3.72 eV for In_2O_3, ITO and SnO_2, respectively. These results are in good agreement with those reported elsewhere [32].

PPy film formation

The *i–t* curves characterizing Py electropolymerization, recorded on G/S electrodes (G: glass, S: In_2O_3, ITO or SnO_2), at potential $E = 1.2$ V/SCE and room temperature, in 0.25 M Py + 0.5 M KCl solution previously deoxygenated and maintained under Ar atmosphere, are shown in Fig. 5. These chronoamperometric curves indicated that the electrode nature exhibited a striking effect on their shape and their characteristics. It can be seen that on In_2O_3 and SnO_2 electrodes, there is solely one peak whose height and position were changed with electrode nature, while two peaks were observed for ITO case. In all cases, The thickness of PPy film was estimated by coulometry using the relationship [33] $e(\mu m) = 2.5Q(C\ cm^{-2})$. The main characteristics were gathered in Table 1.

It is pointed out that [16, 34] the nucleation and growth mechanism of polypyrrole are similar to those suggested for metal. The using of the theoretical model reported for metal growth [35] is, thus, suitable for polypyrrole electropolymerization process. According to this model, the current–time transient characterizing the nucleation of PPy should pass through a maximum whose the presence can be attributed to effect of overlap between growing centres resulting from nuclei formation occured during the first stage of electropolymerization process on active sites on electrode surface. Before overlapping, the currents recorded on In_2O_3 and SnO_2

Table 1 Electropolymerization characteristics of PPy films on various substrates from data in Fig. 5

Substrates	i_{max} (mA cm^{-2})	t_{max} (s)	Thickness (μm)
SnO_2	11.77	10.65	1.85
In_2O_3	10.68	3.05	0.50
ITO			
Peak1	8.11	2.55	0.68
Peak 2	5.89	10.60	

were mainly controlled by these sites that depend only on the substrates nature but remain unchanged with time. Taking into account the i_{max} and t_{max} values in Fig. 5 and Table 1, one can suggest that the number of active sites presented on SnO_2 surface is higher than that resulted from In_2O_3 one, while the growth rate of nuclei formed on later was likely more important than that occured on the former. Concerning ITO, it is solid solution as shown above (Fig. 1). Its chronoamperometric curve (Fig. 5) exhibited two peaks. In former region where $t \leq 2.5$ s, it is likely that the currents were practically originated from nucleation on In_2O_3, owing to the fact that the nuclei formation on these sites is about thrice higher than that occured on SnO_2 with an overlapping time which is more important than In_2O_3 case. On the other hand the $\left(i_{max//ITO}/i_{max/In_2O_3}\right)_{t=t_{max}}$ ratio calculated, using the data of Table 1 and Fig. 5, is 0.76. This allows to suggest that the proportion of In_2O_3 in ITO is about of 76%. After overlapping, the current decrease due to the In_2O_3 sites was compensated by growing of nuclei formed on SnO_2 sites. In this region with $t > 5$ s, the currents recorded on ITO involved two components, $(i_{ITO})_1$ and $(i_{ITO})_2$ regenerated by In_2O_3 and SnO_2 respectively. The SnO_2 content presented in ITO was estimated from the ratio $\left((i_{ITO})_2/i_{SnO_2}\right)_{t=10.6\,s}$, using the experimental data of Fig. 5 and Table 1, which is closed to 0.19. This value indicates that the SnO_2 content in this compound is 19%. This result and the In_2O_3 one are in good agreement with those obtained by EDAX analysis as shown above.

Cyclic voltammetry

The Fig. 6 displays the typical cyclic voltammograms (CVs), recorded on G/S/PPy electrodes (where Ox = In_2O_3, ITO and SnO_2), in pyrrole free 0.5 M KCl solution previously deoxygenated by bubbling argon and maintained under Ar atmosphere. All cyclic voltammograms were performed at room temperature with a scan rate of 10 mV s^{-1} from −0.70 to +0.35 V/ SCE. The change in the shape and characteristics of CVs obtained illustrate a pronounced effect of substrate nature. It can be seen that the increase of the cathodic peak potential, E_{pc}, in sequence In_2O_3 (−292 mV/SCE) < ITO (−160 mV/SCE) < SnO_2 (−133 mV/SCE) always accompanied by a drop of the peak current intensities.

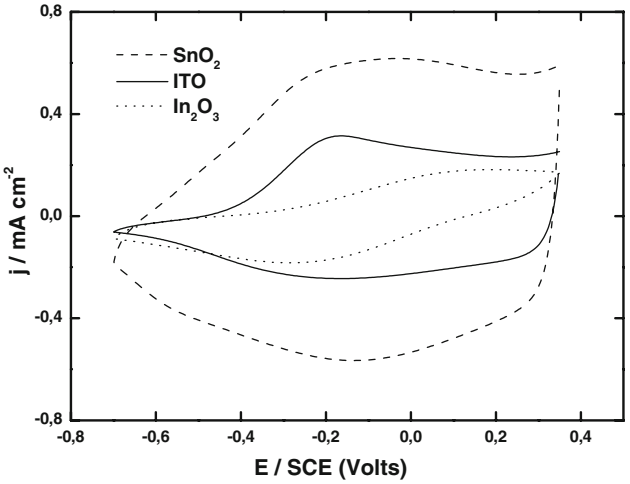

Fig. 6 Cyclic voltammograms (CVs), recorded on G/S/PPy electrodes (where Ox = In_2O_3, ITO and SnO_2), in pyrrole free 0.5 M KCl solution previously deoxygenated, scan rate equalto 10 mV s^{-1}

In its oxidized state the polypyrrole incorporates doping anions in order to neutralize the positive charge (bipolarons) created on its backbone during electropolymerization process. The switching between oxidized and reduced states implies the expulsion/insertion process of doping anion from/into polymer matrix where the moving ability of anion depend not only on its nature [23] but also on the changes in PPy characteristics induced by electropolymerization processes which are controlled by substrate nature, as shown in the chronoamperometric curves (Fig. 5). This explains the change in shape of the CVs. For instance the substitution of In_2O_3 substrate by ITO or SnO_2 ones lead to a positive shift of the cathodic peak potential of 132 and 159 mV, respectively. This indicates that the reduction of PPy formed on In_2O_3 is more difficult than those obtained on other substrates.

It is generally admitted [23, 25, 26] that using Cl^- as doping anion may lead to formation of PPy with a good quality of charge transport, due to its poor nucleophilic character. However, such character may also reduce noticeably the incorporation kinetics of anion into PPy matrix. For the case of PPy formed on In_2O_3, owing to the fact that its nuleation was more rapid than those obtained on other substrates, as shown in Fig. 5, one can expect that a partial doping was occured on this film in which the excess of bipolarons, created on its backbone during electropolymerization, leads to a reduction of Cl^- moving in PPy film. This implies the deterioration of its charge transport characteristics. On the SnO_2 and ITO, the decreasing of PPy formation rate should likely increase its doping level, hence, improves its charge transport characteristics. Such hypothesis is supported by the apparent doping level calculated from a potentiostat equipped integrator. The values are, 4.8%, 7% and 8% for In_2O_3, ITO and SnO_2, respectively.

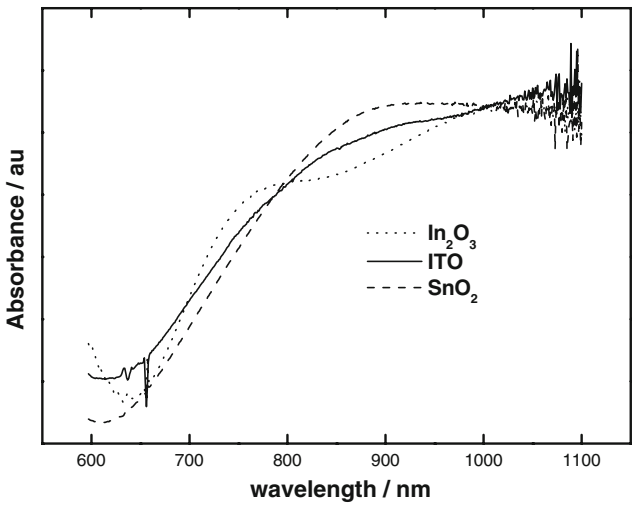

Fig. 7 Absorption spectra of PPy formed on various substrates and nomalized at same thickness

Such hypothesis is also supported by absorption spectra performed on PPy films electrogenerated on In_2O_3, ITO and SnO_2, as shown in Fig. 7. Indeed, it can be seen that spectrum absorption peak recorded on In_2O_3 exhibits a hypsochromic shift in relation with spectra resulted from films formed on other substrates.

Conclusion

It was shown in this investigation that the substrate nature have a striking effect on the charge transport characteristics of PPy flms and their optical properties as well as. Such effect can be attributed to the profound changes in nucleation and growth characteristics of electrogenerated polypyrrole, which are strongly connected to the substrate nature, although the key factors of these modifications are not yet established. The clarifications related to these points appear necessary for an optimization of various electropolymerization characteristics, which should allow to obtain the highly qualities suitable for preparation of thin films by self-assembly.

Acknowledgements This work is part of research program of UMR 7177 CNRS/ULP. The authors acknowledge the support of ECOS/CONICYT (Action C04E02). J.L.G. thanks FONDECYT (project 1050178).

References

1. Leech D (1996) In: Lyons MEG (ed) Electroactive polymer electrochemistry, part 2: methods and applications. Plenum Press, New York, p 268
2. Kuwabata S, Nishizawa M, Martin CR, Yoneyama H (1997) J Electrochem Soc 144:1923. doi:10.1149/1.1837722
3. Leventis J (1988) US Patent 5,457,564
4. Yoneyama H, Shoji Y, Kawai K (1989) Chem Lett 1067. doi:10.1246/cl.1989.1067
5. Chen CC, Bose CSC, Rajeshwar K (1988) J Electroanal Chem 350:161
6. Holdcroft S, Funt BL (1988) J Electroanal Chem 240:89. doi:10.1016/0022-0728(88)80315-2
7. Cosnier S, Innocent C (1992) J Electroanal Chem 328:361. doi:10.1016/0022-0728(92)80195-A
8. Janda P, Weber J (1991) J Electroanal Chem 300:119. doi:10.1016/0022-0728(91)85388-6
9. Rick J, Chou TC (2006) Biosens Bioelectron 22:329. doi:10.1016/j.bios.2006.04.007
10. Nguyen Cong H, El Abbassi K, Chartier P (2000) Electrochem Solid-State Lett 3(4):192. doi:10.1149/1.1390999
11. Nguyen Cong H, de la Guadarrama V, Gautier JL, Chartier P (2002) J N Mat Electrochem Syst 5:35
12. Nguyen Cong H, El Abbassi K, Chartier P (2002) Electrochem J 149(5):A525
13. Nguyen Cong H, de la Guadarrama V, Gautier JL, Chartier P (2003) Electrochim Acta 48:2389. doi:10.1016/S0013-4686(03)00252-4
14. Marco JF, Gancedo JR, Nguyen Cong H, Abbassi KEl, del Canto M, Rios E, Gautier Jl (2008) Mater Res Bull 43:2413
15. Cheng SA, Otero TF (2002) Synth Met 129:53. doi:10.1016/S0379-6779(02)00031-0
16. Hwang BJ, Santhanam R, Lin YL (2000) J Electrochem Soc 147(6):2252. doi:10.1149/1.1393516
17. Nguyen Thi Le H, Garcia B, Deslouis C, Le Xuan Q (2001) Electrochim Acta 46:4259. doi:10.1016/S0013-4686(01)00699-5
18. Ferreira CA, Aeiyach S, Coulaud A, Lacaza PC (1999) J Appl Electrochem 29:259. doi:10.1023/A:1003429401453
19. Cossement D, Plumeir F, Delhalle J, Hevesi L, Mekhalif Z (2003) Synth Met 138:529-0. doi:10.1016/S0379-6779(02)01260-2
20. Rodriguez I, Marcos ML, Gonzalez-Velasco J (1987) Electrochim Acta 32:1181. doi:10.1016/0013-4686(87)80031-2
21. Lee JY, Tan TC (1990) J Electrochem Soc 137:1402. doi:10.1149/1.2086681
22. Martel D, Nguyen Cong H, Molinari M, Ebothe J, Kityk IV (2008) J Math Sci 43:3486
23. Nguyen Cong H, El Abbassi K, Gautier JL, Chartier P (2005) Electrochim Acta 50:1369. doi:10.1016/j.electacta.2004.08.025
24. Rodriguez J, Grande HJ, Otero TF (1997) In: Nalwa HS (ed) Handbook of organic conductive molecules and polymers, vol 2. Wiley and Sons, New York, p 415 and 448
25. Warren LF, Anderson DP (1987) J Electrochem Sci Technol 134:101. doi:10.1149/1.2100383
26. Diaz AT, Bargon J (1986) In: Skotheim T (ed) Handbook of conducting polymer. M. Dekker, New York and Basel, p 81
27. Singh RN, Hamdani M, Koenig JF, Poillerat G, Gautier JL, Chartier P (1990) J Appl Electrochem 20:442. doi:10.1007/BF01076053
28. Restovic A, Poillerat G, Koenig JF, Gautier JL, Chartier P (1991) Thin Solid Films 199:139. doi:10.1016/0040-6090(91)90060-B
29. Ríos E, Poillerat G, Koenig JF, Gautier JL, Chartier P (1995) Thin Solid Films 264:18–24. doi:10.1016/0040-6090(95)06570-9
30. Bouchenaki C (1991) Thèse de Doctorat de l'Université Louis Pasteur, Strasbourg (France)
31. Preusser S, Cocivera M (1987) Sol Energ Mater 15:175. doi:10.1016/0165-1633(87)90064-5
32. Sze SM (1981) Physics of semiconductor devices, 2nd edn. Wiley, New York
33. Diaz AF, Castillo JL, Logan JA, Lee WY (1981) J Elctroanal Chem 129:115
34. Saidman SB, Bessone JB (2002) J Electroanal Chem 521:87. doi:10.1016/S0022-0728(02)00685-X
35. Harisson JA, Thirsk HR (1971) In: Bard AJ (ed) Electroanal Chem, vol 5. Academic Press, New York, p 67